IJST, Transactions of Civil Engineering, Vol. 37, No. C+, pp 437-456
Printed in The Islamic Republic of Iran, 2013

REVEALING THE CHAOTIC NATURE OF RIVER FLOW*

M. H. FATTAHI[1,**] N. TALEBBEYDOKHTI[2], H. MORADKHANI[3] AND E. NIKOOEE[4]

[1]Dept. of Civil Engineering, Marvdasht Branch, Islamic Azad University, Marvdasht, I. R. of Iran
Email: Fattahi_mh@yahoo.com
[2]Dept. of Civil and Environmental Engineering and Head of Environmental Research and Sustainable Development Center, Shiraz University, Shiraz, I. R. of Iran
[3]Dept. of Civil and Environmental Engineering, Portland State University, Portland, Oregon, USA
[4] Dept. of Civil and Environmental Engineering, Shiraz University, Shiraz, I. R. of Iran

Abstract– Chaotic analysis has been performed on the river flow time series before and after applying the wavelet based de-noising techniques in order to investigate the noise content effects on chaotic nature of flow series. In this study, 38 years of monthly runoff data of three gauging stations were used. Gauging stations were located in Ghar-e-Aghaj river basin, Fars province, Iran. Noise level of time series was estimated with the aid of Gaussian kernel algorithm. This step was found to be crucial in preventing removal of the vital data such as memory, correlation and trend from the time series in addition to the noise during de-noising process. A comprehensive chaotic assessment was conducted to study the relationship between the wavelet noise reduction processes and the changes in the chaotic behavior of the river flow time series. To investigate the time series chaotic behavior, some of the most common non-linear criteria are utilized which are distinguished as the chaos indicators. The changes in the signal's average power, the Lyapunov exponents, the correlation dimension and the reconstructed phase space were estimated. Studying the average signals power analysis' results presents the evident impression of de-noising procedure on the river flow time series. The variations of the Lyapunov exponents of time series as a consequence of preprocessing indicated a significant influence of the wavelet based de-noising on revealing the time series chaotic behavior. Results depicted that the lesser noise components result in lowering the largest Lyapunov exponents. Besides, fractal dimension and correlation dimension of the de-noised series were almost the same while they were totally different before de-noising. This also confirmed the commonly claimed sensitivity of correlation dimension to the existence of noise. The correlation dimension results depicted an obvious difference between the signal's chaotic behavior before and after the do-noising procedure. Changes in the reconstructed phase spaces were also noticeable after de-noising process by wavelet techniques. Results confirm the importance of de-noising before any chaotic assessment. Also, results show that a chaotic phenomenon such as river flow may depict completely random behavior due to the noise content within it. Therefore, in order to better explore inherent chaotic behavior of natural time series, such pre-processing can accompany common chaotic assessment procedures.

Keywords– Chaotic behavior, wavelet, noise reduction, river flow

1. INTRODUCTION

Many natural phenomena such as earthquakes, floods, rain, solar radiation and in a wider range, most geophysical events can be studied within the time series framework. Studying natural events as time series gives the ability to investigate their embedded dynamical features in time variant scales. The data driven from natural dynamical systems like observed hydrological time series are prone to noise [1-2]. The measured time series always contain some noise due to random influences (dynamical noise) and

*Received by the editors October 21, 2012; Accepted April 15, 2013.
**Corresponding author

inaccuracies (additive noise) [3]. The performance of modeling techniques, prediction and control of hydrological systems is heavily affected by noise. The chaotic characteristics of time series are also influenced by noise components [4]. As reported in some studies, raw time series of natural events do not show any chaotic deterministic properties until being de-noised [1]. Also, some studies have compared the noise effects on chaotic behavior and predictability of hydrological time series [5]. To reveal the chaotic behavior of the hydrological time series, noise removal or noise reduction is a necessary step. Moving average, low-pass filters, nonlinear smoothing and wavelet-based de-noising algorithms are the common noise reduction techniques [4]. This study focuses on the influence of the wavelet based de-noising techniques and analyzes the chaotic behavior of river flow time series.

Wavelets have been shown to be an indispensable tool for scale variant representation and analysis of temporal data [6]. The suitability of the wavelet analysis roots in its capability in analyzing all types of the signal classes.

Two main classes of signals are the fractional Gaussian noise (fGn) and the fractional Brownian motion (fBm). fGn signals are stationary with an expected mean and constant variance over time and fBm signals are non-stationary with time variant mean and variance. Many natural time series, such as some hydrological time series shade some properties with fBm.

Fourier Transform (FT) and Fast Fourier Transform (FFT) have commonly been used for time series analysis. Employing harmonic sine and cosine transforms repeating constantly in a $(-\infty, +\infty)$ domain, FT and FFT can yield the frequency contents of a signal. However, the Fourier transform is not fully efficient in analyzing the frequency contents of fBm signals [7]. Another deficiency of the Fourier transform is its incapability to determine the occurring time of each frequency beside its amplitude [6]. Although using Short-Time Fourier Transform (STFT), which maps a signal into a two dimensional function of time and frequency can cope with some of these shortcomings, the problem still remains for non-stationary signals.

Wavelet Transform (WT) has overcome the problems working with FFT and STFT. In WT, while analyzing the signal frequency with scale variations, the calculation time will be also reduced significantly. Besides, while the other methods can just analyze the stationary time series, WT efficiently analyze the non-stationary ones as well. Another important feature of WT is its ability to decompose signals at different orders, which is done in a preprocessing step. In wavelet multi-resolution analysis, time series are treated on different scales. WT decomposes the signals into coefficients of coarser scales defining approximation signals and coefficients of finer scales, the so-called detail signals. Decomposing a signal into the approximation signal, revealing the signal's basic trend, and the detail signal indicating the noise components, is an effective technique in data processing as it leads to noise separating approach. WT provides a mechanism to exclude the noise term from the signal or reduce it to a level which does not affect the time series predictability or chaotic behavior remarkably if it possesses any. Continuous Wavelet Transform (CWT) and Discrete Wavelet Transform (DWT) are two wavelet approaches to perform the noise removal.

Although stochastic models are indispensable tools for studying geophysical systems some hydrological processes are not as irregular and complex to be distinguished as random systems (high dimensional) and to be treated with the limitations of the stochastic models [5]. Hydrological processes studied by some researchers [8-16], which have shown low chaotic dimensionality, are assumed to be chaotic systems. These non-linear dynamic systems might be better understood if we use non-linear chaotic models to analyze them instead of stochastic ones [17].

The chaotic behavior of the stream flow time series has been investigated by many researchers [12-21]. Some studies have demonstrated that chaotic approach is better than the traditional stochastic approaches for analyzing dynamic hydrological systems [22-24]. However, the effect of the wavelet based

de-noising techniques on the chaotic behavior of the river flow time series has not yet been fully explored and understood.

The special feature of this study is the comprehensive analysis of wavelet based noise reduction effects on the different chaotic aspects of the time series. The chaotic assessments based on the signal power spectrum, Lyapunov exponent, correlation dimension and reconstructed phase space have been used to explore the variations in chaotic behavior of time series due to wavelet based de-noising.

It is worth mentioning that while the effects of de-noising on chaotic behavior of the time series in fundamental point of view is nothing new, however, to the best of the authors knowledge the current study has this positive point in comparison to the other similar works in the literature, which favor determination of the noise level based on the noise effects on the chaotic characteristics of the time series and then de-noising the time series in a controlled manner; this has then ended in revealing the chaotic nature of time series in a better way. This means that for the reason that noise level estimation has been done prior to de-noising and noise level estimation has itself been performed based on the noise effects on the dynamic of the time series, the offered procedure is an integrated approach. This approach, therefore, is of great benefit in conventional chaotic analysis of time series in hydrologic sciences as it offers a systematic way to determine noise level, pre-process the time series and finally to perform the chaotic post processing.

2. THEORY

a) Wavelet analysis

Wavelet concept provides a method to overcome the limitations of Fourier analysis. Fourier analysis consists of breaking up a signal into sine waves of various frequencies while wavelet analysis is the breaking up of a signal into shifted and scaled version of the original wavelet which is called the mother wavelet [25]. Clearly a signal with sharp edges and changes would be better analyzed with an irregular wavelet than with a smooth sinusoid. Employing WT, time information and frequency contents of a signal can be accessed simultaneously, in other words, wavelet transform is a time-frequency representation of a signal.

The mother wavelet should have properties that lead to a meaningful interpretation of the decomposition [6]. It should be able to split the signal recursively into a trend and a fluctuation called approximation and detail signals. The smooth part of the time series is the actual trend (approximation) in each time scale and the residuals or fluctuations are the noise (detail).

The CWT of a function f is an integral transformation of the form

$$\left(w_{\psi} f\right)(a,b) = \int_{R} f(x)\psi_{a,b}(x)dx, \tag{1}$$

In which a is scale and b is the translation parameter that depict the location. $\psi_{a,b}(x)$ is defined by

$$\psi_{a,b}(x) = \frac{1}{\sqrt{|a|}}\psi\left(\frac{x-b}{a}\right) \tag{2}$$

This transformation is called continuous because a and b are real numbers. Applying the CWT to a function f for different pair of parameters a and b make different information on f. Therefore, after the wavelet decomposition the signal frequency can be obtained at different scales.

The CWT is useful for theoretical purposes but for practically analyzing signals it is not a suitable choice. It needs a great amount of computation time and resources. The DWT which corresponds to the

transform Eq. (1) for discrete values of *a* and *b*, reduces the computation time significantly and is simpler to implement. It is defined as follows:

$$f(t)=\sum_{j=-\infty}^{\infty}\sum_{k=-\infty}^{\infty}d_k^j\psi_{j,h}(t) \tag{3}$$

In which the coefficients are determined as

$$d_k^j=\int_R f(t)\psi_{j,k}(t)dt \tag{4}$$

This could be achieved if we represent the wavelet as

$$\psi_{j,k}(t)=\frac{1}{\sqrt{\left|a_0^j\right|}}\psi\left(\frac{t-kb_0a_0^j}{a_0^j}\right) \tag{5}$$

where $a_0>1$ is a fixed dilation step and the translation parameter b_0 depends on the dilation step. Both CWT and DWT are used to decompose the signals as the data preprocessing. The signals are conducted through high pass and low pass filters of different frequencies. The signal is then decomposed to one containing the high frequencies, which indicates the signal's noise (the detail) and the rest is the trend (the approximation). This filtering course of action continues and in the next level the approximation signal is decomposed into noise and trend signals through the same procedure. Depending on the level of decomposing, the procedure repeats till a defined frequency is removed from a specific part of the signal.

b) Chaotic assessment tools

1. Power Spectral Density (PSD) analysis: The PSD method is used for evaluating the fractal properties of time series and is based on the bias of the periodogram attained by the Fast Fourier Transform (FFT) algorithm. A time series can be analyzed in the frequency domain using the PSD which is the signal power representation within the frequency band. The presented relation by Mandelbrot and Van Ness for the self-affine fractals [26] is expressed in the frequency domain as follows:

$$S(f)\propto 1/f^{\beta} \tag{6}$$

Where f is the frequency and $S(f)$ the correspondent squared amplitude. By calculating the negative slope $(-\beta)$ of the line relating $\log(S(f))$ to $\log(f)$ one can estimate β. For fGn series β exponents ranging from -1 to +1 and the range for fBm vary between 1 and 3. Hurst exponent can be obtained through β using the following equations:

$$H=\frac{\beta+1}{2} \qquad \text{for fGn time series} \tag{7}$$

$$H=\frac{\beta-1}{2} \qquad \text{for fBm time series.} \tag{8}$$

As reported by the author the length and class of time series have a direct influence on the fractal analyzing tool [27]. The PSD method is chosen for its adaptation with the nature of the flow time series that are applied in this research according to the given flowchart [27]. The power spectral density is utilized for the time series continuous spectrum. The integral of the PSD over a given frequency band computes the average power in the signal over the frequency band. The power spectral density of a

random process X_n is mathematically related to the correlation sequence by the discrete-time Fourier transform. In terms of normalized frequency, it is given by

$$P_{xx}(\omega)=\frac{1}{2\pi}\sum_{m=-\infty}^{\infty}R_{xx}(m)e^{-j\omega m} \tag{9}$$

As a function of physical frequency f, using the relation $\omega=2\pi\cdot f/f_s$ in which f_s indicates the sampling frequency, we get

$$P_{xx}(f)=\frac{1}{f_s}\sum_{m=-\infty}^{\infty}R_{xx}(m)e^{-2\pi jfm/f_s} \tag{10}$$

The average power of a signal over a particular frequency band $[\omega_1,\omega_2], 0\le\omega_1<\omega_2\le\pi$, can be obtained by integrating the PSD over that band in which $p_{xx}(\omega)$ represents the power contents of a signal in an infinitesimal frequency.

$$\overline{P}_{[\omega_1,\omega_2]}=\int_{\omega_1}^{\omega_2}P_{xx}(\omega)d\omega+\int_{-\omega_2}^{-\omega_1}P_{xx}(\omega)d\omega \tag{11}$$

It is important to note that the estimated power is the average power not the peak power.

2. Phase space reconstruction: A time series is composed of a long-term trend plus various periodic and random components. The apparently random components of a time series can be truly random whereby the measurements are based on some underlying probability distribution or they may not be random at all, but rather, chaotic[28].

Although a chaotic time series appear to be randomly distributed and non-periodic, it is actually characterized by the values that are the result of a completely deterministic process. In fact, chaotic time series display some stochastic conducts in time domain and depict some determined behavior in embedding phase space [28]. An important step in analyzing the chaotic behavior of any dynamic system is to reconstruct the phase space of the time series. The trajectories of a phase space depict the evolution of a dynamic system from some initial known state and therefore represent the history of the system [29]. The concept of embedding a single-variable series in a multi-dimensional phase space is the key to revealing the underlying chaotic dynamics. The method employed to reconstruct the phase space is the method of delays [30-32]. Accordingly, for a hydrological time series such as a stream flow series, X_i, in which $i=1,2,...,N$, and its successive delays as coordinates of a new vector time series the reconstructed phase space would be presented as

$$Y_t=\{x_t,x_{t-\tau},x_{t-2\tau},...,x_{t-(m-1)\tau}\} \tag{12}$$

where τ indicates the delay time and m is the embedding dimension term. The embedding dimension is the adequate dimension for recovering the geometric object without deforming any of its topological properties. Each point in the phase space represents the state of the dynamic system at a given time.

3. Estimating the Lyapunov exponent: One criterion to characterize a chaotic conduct quantitatively is the Lyapunov exponents. The growth or the shrinkage rate of small perturbations in different directions in the phase space is described with Lyapunov exponent in a logarithmic scale [33]. Lyapunov exponents measure the average exponential divergence or convergence between trajectories (geometric objects which characterize the long-term conduct of a system in the phase space [12]) that differ only in having infinitesimal differences in their initial conditions and remain well defined for noisy systems [34].

Imagine a set of initial conditions within a sphere or radius ε in phase space. For chaotic motions, trajectories originating in the sphere will map the sphere into an ellipsoid whose major axis grows as

$d = \varepsilon \cdot e^{\lambda \cdot t}$, where $\lambda > 0$ is known as a Lyapunov exponent. For regular motions $\lambda \le 0$ but for chaotic motions $\lambda > 0$. Thus, the sign of λ is a criterion for chaos. If d is the maximum length of the ellipsoid and d_0 is the initial size of the initial condition sphere, Lyapunov exponent λ is interpreted by the equation

$$d = d_0 2^{\lambda(t-t_0)} \tag{13}$$

The average of the calculation over different regions of phase space is represented by

$$\lambda = \lim_{N\to x} \frac{1}{N} \sum_{1}^{N} \frac{1}{(t_i - t_{0i})} \log_2 \frac{d_i}{d_{0i}} \tag{14}$$

The diversity of noise existing in natural time series makes it difficult to find the exact Lyapunov exponent. The largest Lyapunov exponent is calculated based on the algorithm introduced by Rosenstein et al. [32]. The algorithm express λ as follows: let $x(\tau)$ be the time evolution of the initial condition $x(0)$ in a suitable state space. The largest Lyapunov exponent can be estimated then by

$$\lambda = \lim_{\tau\to\infty} \lim_{\varepsilon\to 0} \frac{1}{\tau} \ln\left(\frac{\left|x(\tau) - x_\varepsilon(\tau)\right|}{\varepsilon}\right),$$
$$\left|x(0) - x_\varepsilon(0)\right| = \varepsilon \tag{15}$$

As stated a positive λ indicates the presence of chaos and the negative λ indicates on non-conservative systems [35]. There are many algorithms to calculate the Largest Lyapunov Exponent (LLE) as the strongest identity of the chaos. According to the proposed algorithm by Rosenstein et al., to find the LLE one should calculate the following relation:

$$S(\Delta t) = \frac{1}{N} \sum_{t_0=1}^{N} \ln\left(\frac{1}{\left|U\left(s_{t_0}\right)\right|} \sum \left|S_{t_o+\Delta t} - S_{t+\Delta t}\right|\right) \tag{16}$$

S_{t_0} is the reference point (embedding vector) and $U(S_t)$ is the neighborhood of S_{t_0} with diameter ε. LLE is calculated studying the slop of $S(\Delta t)$ when it shows a linear increase for all reasonable values of ε and all embedding dimensions, m.

We would analyze and compare the chaotic behaviors of signals using the Lyapunov exponent criterion as used by [35] before and after the signal decomposition to inspect the probable changes in the signals' perturbation whether they contain noise and random components or not.

4. Correlation dimension analysis: Correlation dimension algorithm is presented by Grassberger and Procaccia [36] for the first time. It expresses the dynamics of a system upon its relevant time series using the phase space concept. The correlation dimension stated as D_2 quantifies the complexities and irregularities of the reconstructed system. Correlation dimension algorithm works well for noise free data sets but for noisy systems the estimations are absolutely unreliable. The estimate of D_2 of a noisy data set does not converge with increasing m but D_2 of a chaotic system converges to a finite value as m grows. The correlation dimension can be calculated from a time series by

$$D_2 = \lim_{\varepsilon\to o} \frac{\log C(\varepsilon)}{\log \varepsilon} \tag{17}$$

Where ε is the radius around Y_t and the correlation integral $C(\varepsilon)$ depicts the probability that two vectors on the attractor are separated by a distance smaller than a radius ε. The correlation integral is defined by

$$C(\varepsilon) \equiv \lim_{N\to\infty} \frac{1}{N^2} \sum_{i,j=1}^{N} H(\varepsilon - |Y_i - Y_j|), \qquad u = \varepsilon - |Y_i - Y_j| \tag{18}$$

In which $H(u)$ is the Heaviside step function where $H(u) = \begin{cases} 1 & x > 0 \\ 0 & x \le 0 \end{cases}$. The number of points in the vector Y_t is N and ε is the distance. If the mentioned time series can be described by an attractor then the correlation integral and the radius would be related as

$$C(\varepsilon) \approx \alpha \varepsilon^{D_2} \tag{19}$$

In which α is coefficient and D_2 is the correlation dimension. The slope of the linear portion in the plot of $\log C(\varepsilon)$ vs. $\log \varepsilon$ would estimate D_2. Chaos can be detected within a time series through plotting the correlation dimension versus the embedding dimension. For random processes D_2 increase linearly with increasing the embedding dimension but chaotic systems depict a saturation value for D_2. If D_2 reaches a constant value for a defined value of m (saturation value) the system is assumed to be chaotic. Correlation dimension, as a chaotic assessment tool, is employed to investigate the chaotic behavior of the river flow time series before and after the wavelet based noise reduction processing.

c) Noise level estimation

Noise is almost always present in real data sets. The first and most important step before noise reduction is presenting a method for the estimation of noise level. The estimation of noise is basically the estimation of its standard deviation. Presence of the noise can strongly affect chaotic behavior of time series and can influence performance of the prediction techniques. The imprints of noise can be found when dealing with the determination of correlation integral for natural time series. Eq. (18) is generally appropriate for noise free signals. Noise tends to increase the slope of $C(\varepsilon)$ vs. ε in the log-log plot. This slope for a noise free time series and for small values of ε is constant and is equal to the correlation dimension of the time series. The presence of noise strongly affects the correlation integral. One of the main contributions to the investigation of the effect of noise on correlation integral was made by Schreiber [37] who used maximum norm to define correlation integral and obtained the following equation for the correlation integral of time series infected with Gaussian noise.

$$\frac{d[\ln(C_{m+1}(\varepsilon))]}{d[\ln(\varepsilon)]} = \frac{d[\ln(C_m(\varepsilon))]}{d[\ln(\varepsilon)]} + \frac{r \exp(-r^2/4\sigma^2)}{\sigma\sqrt{\pi}.erf(r/2\sigma)} \tag{20}$$

where σ is the standard deviation of the Gaussian distribution, and "erf" denotes the error function, and m specifies the embedding dimension.

A simpler form for the correlation integral has been presented by Schouten et al. [38]. It is also based on the maximum norm. Using the upper bound of radius ε as ε_0 and δ as the maximum noise amplitude they have obtained the correlation integral as follows:

$$C_m(\varepsilon) = \left[\frac{\varepsilon - \delta}{\varepsilon_0 - \delta}\right]^D \qquad \delta \le \varepsilon \le \varepsilon_0 \tag{21}$$

In fact, correlation integral can also be measured using Euclidian norm [39] or a Gaussian kernel [40]. Each form can then be utilized to determine the correlation integral in the presence of noise. The final relationships for correlation integral usually contain correlation dimension and the standard deviation of noise which can be determined by a nonlinear regression technique. Yu et al. [41] has presented an efficient implementation for the Gaussian kernel estimation algorithm to obtain the noise level from noisy data. As demonstrated, the method is computationally efficient and can give reasonable estimations for the standard deviation of noise, [41].

The Gaussian kernel correlation integral $T_m(h)$ for the noise-free case scales is:

$$T_m(h) = \int dx.\rho_m(x) \int dy.\rho_m(y).e^{-\|x-y\|^2/4h^2} \approx e^{-mK\delta t}\left(\frac{h}{\sqrt{m}}\right)^D \quad h \to 0\ , m \to \infty \tag{22}$$

where D and K are the correlation dimension and entropy, h ,is referred to as the bandwidth, and $\rho_m(x)$ is the distribution function. In the presence of Gaussian noise, the distribution function $\rho_m(y)$ can be expressed in terms of a convolution between the underlying noise-free distribution function $\rho_m(x)$ and a normalized Gaussian distribution function with standard deviation σ .

$$\rho_m(y) = \int dx\rho_m(x).\rho^g{}_m(\|y-x\|) = \frac{1}{\left(\sigma\sqrt{2\pi}\right)^m} \int dx\rho_m(x).e^{-\|y-x\|^2/2\sigma^2} \tag{23}$$

Under conditions (21) and (22), the Gaussian kernel correlation integral $T_m(h)$ in the presence of Gaussian noise and the corresponding scaling law becomes:

$$T_m(h) = \int dx\rho_m(x).e^{-\|x-y\|^2/4h^2} = \left(\frac{h^2}{h^2+\sigma^2}\right)^{m/2} \int dx\rho_m(x) \int dy\rho_m(y).e^{-\|x-y\|^2/4\left(h^2+\sigma^2\right)} \tag{24}$$

Considering ϕ as a normalized constant the Gaussian kernel correlation integral is calculated as follows:

$$T_m(h) = \phi\left(\frac{h^2}{h^2+\sigma^2}\right)^{m/2} e^{-mK\delta t}\left(\frac{h^2+\sigma^2}{m}\right)^{D/2} \sqrt{h^2+\sigma^2} \to 0\ , m \to \infty \tag{25}$$

In which σ is referred to as the noise level and is defined as:

$$\sigma = \frac{\sigma_n}{\sigma_s} = \frac{\sigma_n}{\sqrt{\sigma_c{}^2 + \sigma_n^2}} \tag{26}$$

In which σ_n , σ_c and σ_s are the standard deviations of the input noisy signal.

In the present study Gaussian kernel estimation method as presented by Yu et al. [41] has been used to estimate the standard deviation of noise and the noise level of time series. Following the same definition as the one made by Yu et al. [41] for the noise level, thereafter, noise level is considered as the ratio of the estimated standard deviation of noise to the standard deviation of noisy time series. In the present study, based on the estimated standard deviation of noise (noise level), number of de-noising stages using the wavelet technique was determined. The estimated noise level is used to control the amount of details which wavelet de-noising techniques removes from the noisy time series. The standard deviation of removed details (the cumulative sum of the removed details up the level in which noise level is supposed to calculate is considered) should not be more than the estimated noise level to avoid removal of a part of

clean time series (original signal). This way we control that part of the original series which is going to be removed in order not to contain significant information that affects the series natural essence. Further control can be done by analyzing the chaotic dynamics of the time series before and after applying de-noising technique.

3. RESULTS AND DISCUSSION

a) Study site description

Ghar-e-Aghaj river flow basin located in Fars province in Iran was chosen as the case study. Thirty eight years of monthly recorded stream flow data (1971-2009) from three gauging stations in the site area have been used for this research. The selected gauging stations were Band-e-Bahman station, Aliabad station and Tang-e-Karzin station. The river's basin has a half mountainous half plane nature and its area exceeds 3000 km^2. The river's basin and the selected gauging stations have been shown in Fig. 1.

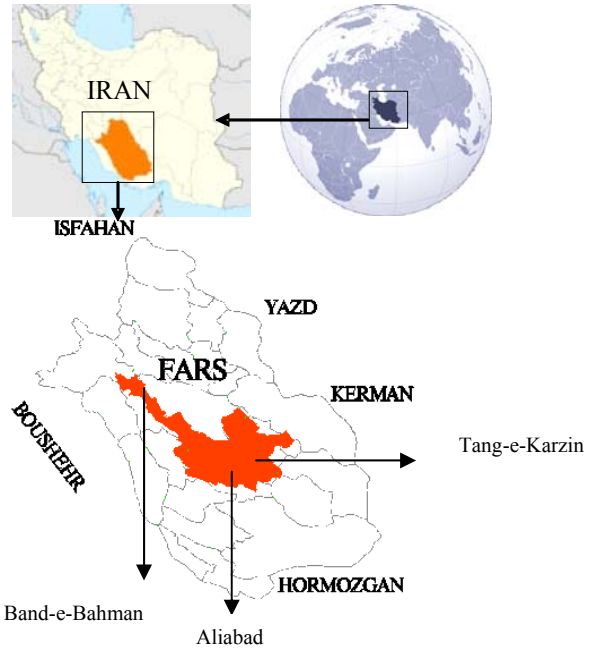

Fig. 1. Ghar-e-Aghaj River basin in Fars province Iran, and Band-e-Bahman, Aliabad and Tang-e-Karzin gauge stations

b) Results of the noise level estimation and wavelet based de-noising

In order to de-noise the studied river flow time series both CWT and DWT techniques were used. The CWT based approximation and detail signals are depicted in Figs. 2a-b. In the present study, the noise level estimation and, subsequently, de-noising were pursued for all considered stations. The different stations showed different behavior dealing with the noise level estimation, i.e., the estimated noise level in Band-e-Bahman station was equal to 0.3922 where in Tang-e-Karzin it was 0.448. Therefore, the de-noising processes continued 9 levels in Tang-e-Karzin and just 2 levels for Band-e-Bahman station to de-noise the signal up to the estimated noise level. In fact, the standard deviation of the detail signal in the corresponding de-noising stage was controlled.

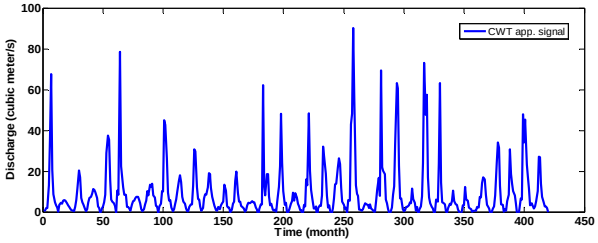

(a)

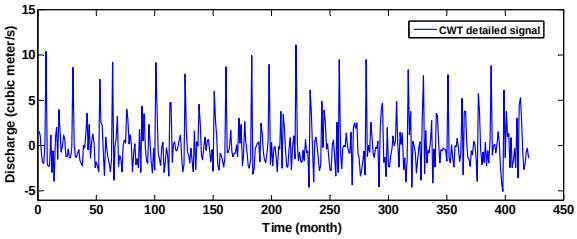

(b)

Fig. 2. Signal decomposing into the approximation and the detail signal using CWT transforms. (a) Band-e-Bahman CWT based approximation signal. (b) Band-e-Bahman CWT based detail signal.

This value should not exceed the estimated noise standard deviation. At each level of de-noising that this constraint is satisfied, the level is supposed to be an allowable de-noising level. In the present study the allowable de-noising level is calculated according to the noise level that the Gaussian kernel estimation algorithm yields. Results depicting the noise level and the corresponding de-noising stage are presented in Table 1.

Table 1. Noise level estimation for the three stations

Station	Noise		Denoising level	Standard deviation of detail signal
Band-e-Bahman	Noise level	0.3922	1	2.707
	Estimated standard deviation	5.6625	2*	4.42
			3	6.17
Aliabad	Noise level	0.3385	1	2.368
	Estimated standard deviation	6.348	2	4.079
			3*	5.433
			4	6.636
Tang-e-Karzin	Noise level	0.448	1	2.501
	Estimated standard deviation	13.1082	2	4.458
			3	6.367
			4	7.88
			5	9.2
			6	10.37
			7	11.48
			8	12.05
			9*	12.95
			10	13.87

* denotes the last allowable de-noising stage where the estimated standard deviation of noise is equal or more than that of the detail signal which would be removed from the main signal. The detail signal is a part of the signal which is obtained after de-composition process, in each stage, by Wavelet based de-noising technique and can be considered as noise. This procedure is to assure part of the main signal is not removed instead of the noise.

The variation of the noise level and the estimated standard deviation of noise with embedding dimensions can also be found in Figs. 3a-b. As it can be seen for large embedding dimensions the curve approaches a fairly constant value for the standard deviation of noise and the noise level which have been considered for determination of the de-noising level based on the wavelet technique.

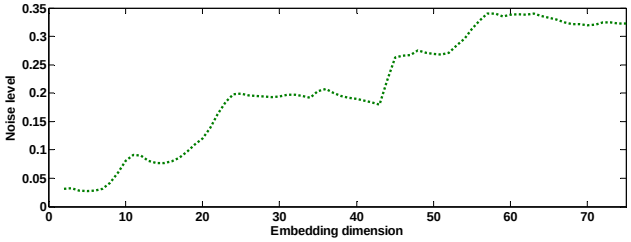

(a)

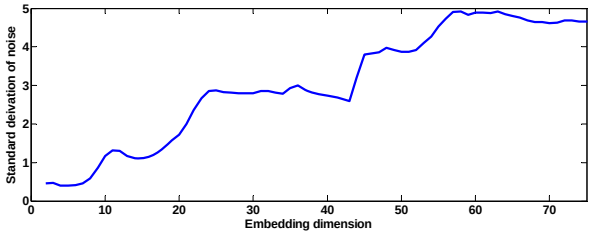

(b)

Fig. 3. (a) Variation of the noise level vs. the embedding dimension (b) Variation of the standard deviation of the noise vs. embedding dimension

c) Results of the power spectral density as well as average signal power analysis

The PSD analysis has been preformed to obtain the Hurst exponent of the time series of the original signals as well the CWT and DWT (de-noised) signals (Figs. 4a-c). The average power has also been obtained for the aforementioned signals (Figs. 5a-c).

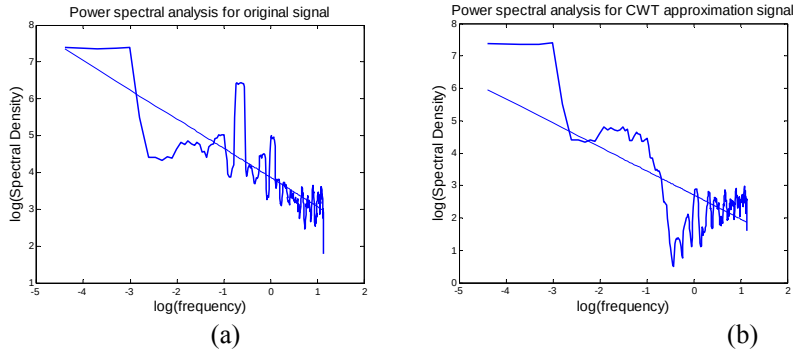

(a)

(b)

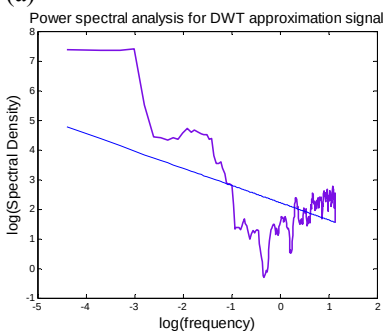

(c)

Fig. 4. PSD analysis and the Hurst exponent calculation. (a) PSD analysis for Band-e-Bahman original time series. (b) PSD analysis for Band-e-Bahman CWT approximation signals. (c) PSD analysis for Band-e-Bahman DWT approximation signals

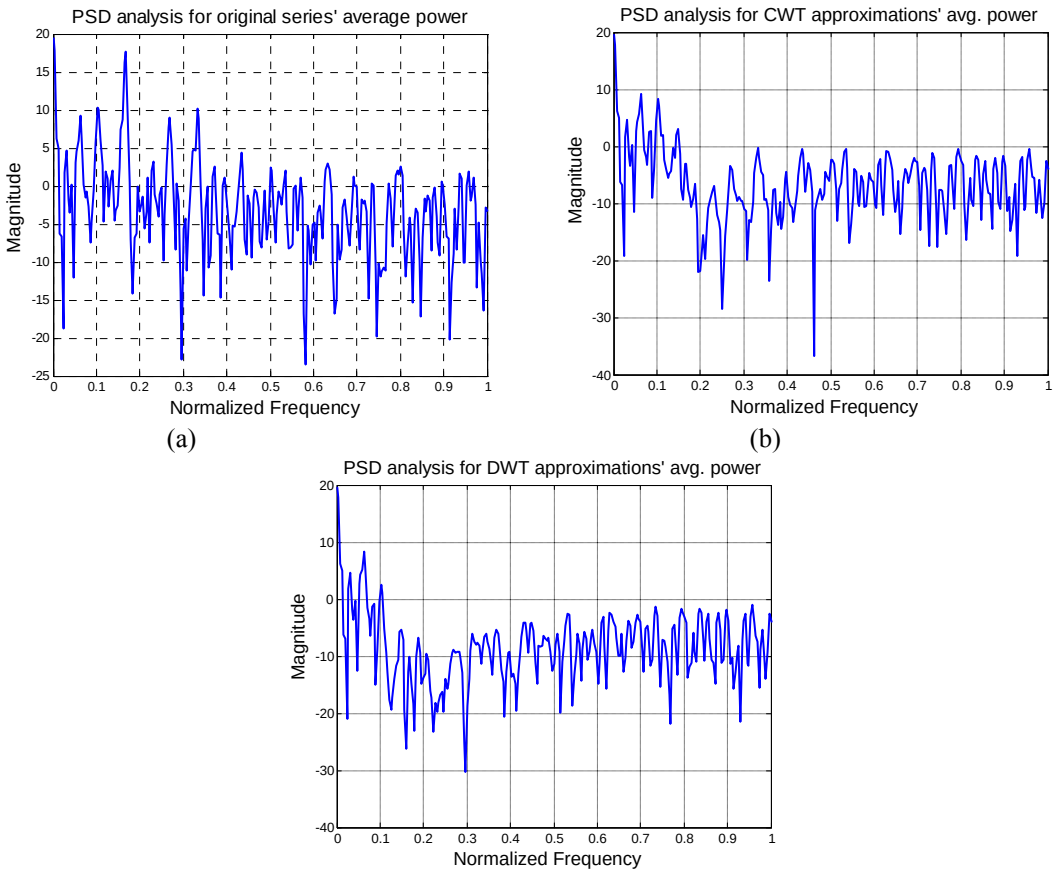

Fig. 5. Average signal power analysis (a) Average signal power for the original time series of Band-e-Bahman station (b) Average signal power for CWT approximation signal of Band-e-Bahman station (c) Average signal power for DWT approximation signal of Band-e-Bahman station

The average signal power variations due to decomposition (de-noising) are completely remarkable. Studying the changes in the average power showed that a considerable amount of the signal's total energy is the noise energy which signifies the irregularities like jumps or sharp spikes in the original signal. Moreover, the signals average power and correlation seemed to have an inverse relationship. Actually, wavelet based de-noising procedures which result in the energy reduction in the signal can potentially lead to an increase in the signal's long term memory.

d) Results of the phase space reconstruction

The phase space patterns of the time series have been depicted before and after decomposing by CWT and DWT techniques in Figs. 6a-c.

Therefore, it can be seen that the chaotic behavior of the signals is under the influence of decomposing process. The random behavior embedded in the signal phase space pattern tended to chaotic one after the signal decomposition (de-noising). The signals' trend was more clarified when the random components of time series were removed. This is traceable through the Lyapunov exponents as well as the phase space pattern. As it can be understood from Fig. 6a-c, the phase space patterns of CWT and DWT approximation signals, while being very similar to each other, are remarkably different from the original signal's phase space pattern. The chaotic behavior can be easily distinguished in the de-noised signals' pattern, especially in contrast to the random behavior of the original signal's phase space pattern.

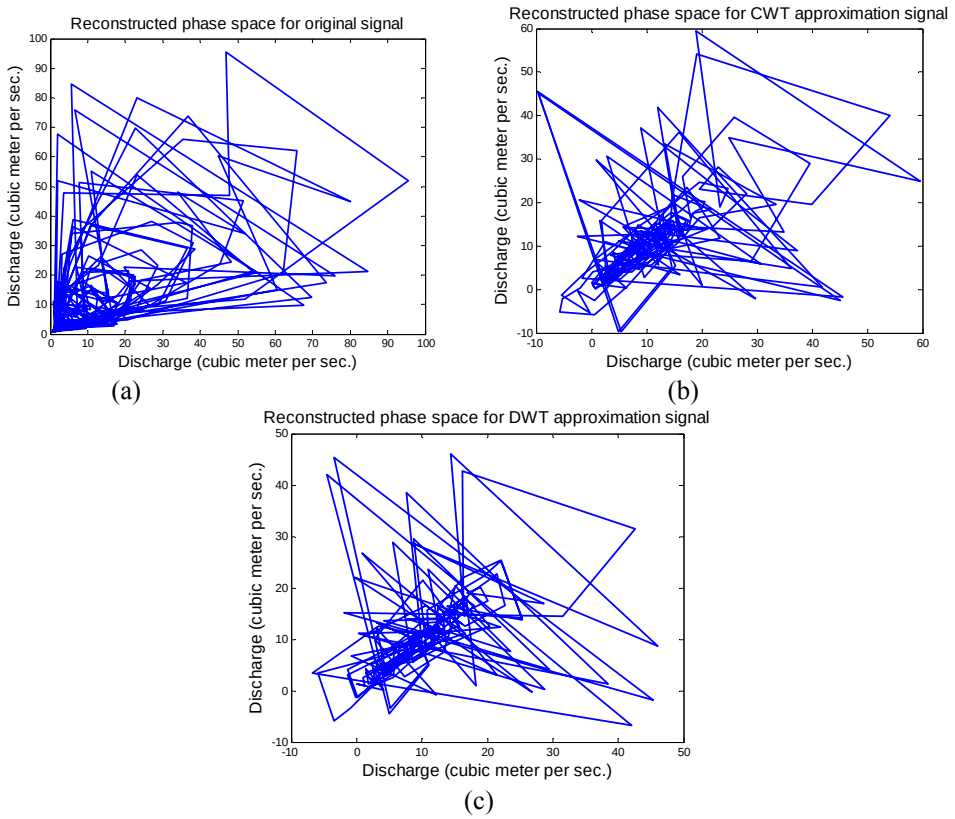

Fig. 6. Phase space patterns for the three scenarios. (a) Reconstructed phase space of Band-e-Bahman original signal. (b) Reconstructed phase space of Band-e-Bahman CWT approximation signal. (c) Reconstructed phase space of Band-e-Bahman DWT approximation signal

Mapping time series data into a phase space allows one to view the temporal series in a spatial manner. One of the most interesting procedures for checking the presence of chaos is based on the ability of recovering the attractor of a system in the phase space. The size of a pattern (i.e., an attractor) is one of the critical factors that governs the accuracy of prediction. A smaller magnitude of fluctuating trajectories in the phase space can reduce the uncertainty in the projectile facing the target dimension. Another factor that governs the accuracy of prediction is the orientation of a pattern. For example, when the prediction is considered along the "y" dimension only, a unique and precise projectile instruction pointing to the estimation side (i.e., y-dimension) is determined. Therefore, the orientation of a pattern with wide input facing along the x-dimension and limitation on the projectile facing along the y-dimension would not give sufficient information about the process. Such an orientation seriously affects the prediction accuracy. Thus, it can be concluded that a seemingly strange attractor is not always capable of providing a less mean square error of prediction; the size and the orientation of a pattern may impair its predictability.

Accordingly, the phase space pattern of the original signal which is obviously larger in size than the other two constructed phase spaces demonstrates more uncertainty elements in its map and can be assumed to be less predictable. Moreover, its orientation pattern in the phase space depicts a scattered behavior in both x and y dimensions, while for the phase spaces developed for processed signals a kind of regularity and a tendency to be ordered through the dimensions can be detected.

e) Results of Lyapunov exponent' estimation

The Lyapunov exponents' variations of the preprocessed time series depict remarkable difference of the original signals. A distinguishable decrease in the Lyapunov exponents' values of the de-noised series from the original time series was detected. A similar consequence has been reported by some other researchers [42-45] in terms of Lyapunov exponents increasing under the influence of noise. Results indicated a direct relationship between WT preprocessing procedure and the decrease in the Lyapunov

exponent's values. Similar to the phase space pattern the Lyapunov exponents' variations of CWT and DWT approximation signals were slightly different. The results indicating the variations in the signals' chaotic behavior, expressed as the changes in Lyapunov exponent, have been shown in Table 2. Using the Rosenstein et al. algorithm, LLE is calculated for the three signals (original one, de-noised by CWT and de-noised by DWT). The variations of $S(\Delta t)$ with time for different embedding dimensions are depicted in Figs. 7a-c. The maximum Lyapunov exponent for the original signal is calculated as LLE=0.2583, for the CWT approximation signal LLE=0.0889 and the least λ is calculated for DWT based approximation signal. LLE=0.0742 in this case. Largest Lyapunov Exponent being positive indicates that the river flow posses a chaotic behavior. The lower (the less positive) the value of LLE is, the more predictable the signal would be. Actually, LLE has an inverse relation with the predictability. Thus, it can be claimed that the predictability of the original signals is about 3.87 months, while for the CWT based preprocessed signal this range is about 11 months and for the DWT based preprocessed signals it is close to 14 months.

Table 2. Variations of the Largest Lyapunov exponents of the river flow time series after the preprocessing procedure

Station	Lyapunov exponent Original signal	Lyapunov exponent DWT approximation signal	Lyapunov exponent CWT approximation signal
Band-e-Bahman	0.2583	0.0724	0.0889
Aliabad	0.3146	0.0854	0.0917
Tang-e-Karzin	0.512	0.1219	0.1613

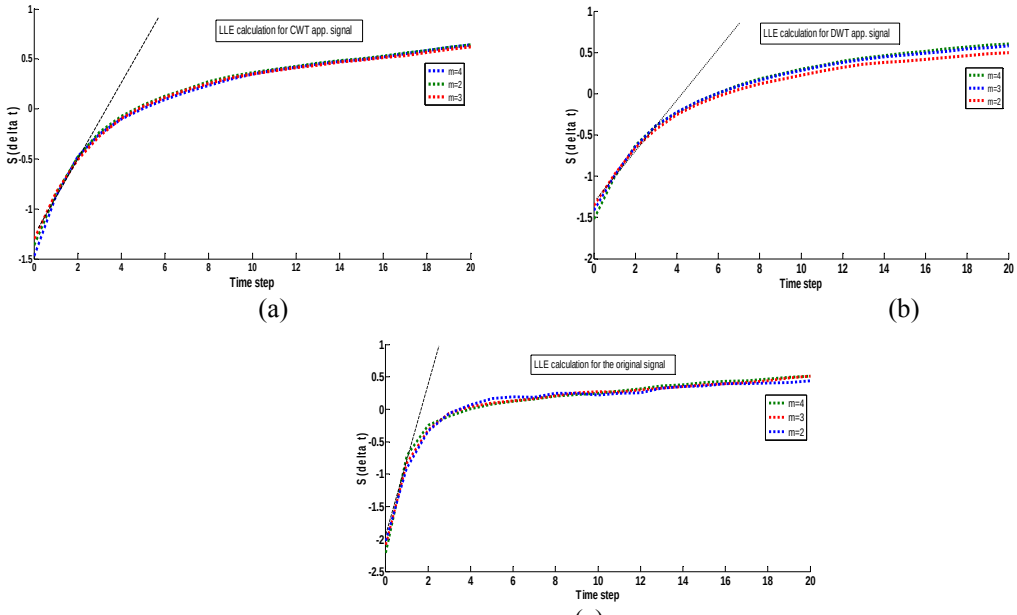

Fig. 7. Variation of $S(\Delta t)$ with time for various embedding dimensions
(a) Scenario 1, (b) Scenario 2 and (c) Scenario 3

f) Results of the correlation dimension analysis

Although fractal dimension is the most important measure of a set [44] and leads to an evaluation of the number of local directions available to a system [22], when dealing with a noisy system like most practical time series, a more noise sensitive tool like correlation dimension seems necessary as well. The correlation integral $C(\varepsilon)$ according to Grassberger and Procaccia [36] algorithm is calculated for embedding dimensions m=2-20. Figs 8a-b show a plot of correlation integral $C(\varepsilon)$ versus radius ε on a log–log scale for embedding dimension m=2-20. The correlation exponent is determined by the slope of the plot of $C(\varepsilon)$ versus ε on a log–log scale [46].

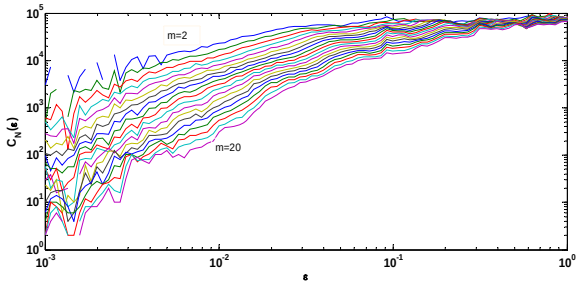

(a)

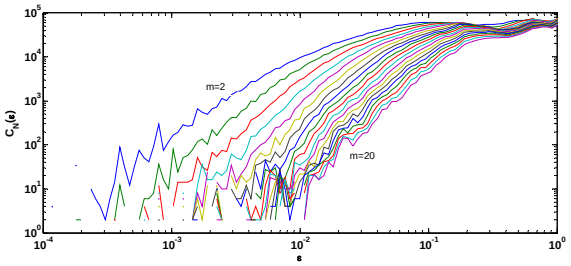

(b)

Fig. 8. Variation of correlation integral with radius on a log–log scale for embedding dimensions from m=1-20. (a) DWT based app. Signals of Band-e-Bahman station. (b) DWT based app. Signal of Aliabad station

Results of the correlation dimension and its comparison to the fractal dimension are illustrated in Table 3. The correlation dimension analysis done in the present study elaborately confirmed that the correlation dimension is more sensitive than fractal dimension to the existence of noise. Results show that while the fractal dimension, D_f, of time series does not show a great variation before and after de-noising, the correlation dimension, D_2, of time series varies remarkably after de-noising. Fractal dimension and the correlation dimension calculated for the de-noised time series were almost the same but for noise contained datasets the two were completely different. Therefore, noise reduction must precede the computation of the invariant measures.

Table 3. Variations of the correlation dimension of the river flow time series due to DWT based de-noising processes as well as comparison with the changes in fractal dimension

Station	D_f Original signal	D_f DWT based approximation signal	D_f CWT based approximation signal	D_2 Original signal	D_2 DWT based approximation signal	D_2 CWT based approximation signal
Band-e-Bahman	1.55827	1.18173	1.21588	0.83	1.1509	1.1032
Aliabad	1.56581	1.21304	1.24782	0.7845	1.0971	1.1736
Tang-e-Karzin	1.51426	1.11021	1.157	0.7644	1.0889	1.1167

To study the variations of the correlation dimension one can plot correlation dimension vs. the embedding dimension. In the present study, the correlation dimension for embedding dimensions m=1-20 and for two gauging stations in two time scales of monthly and weekly discharge have been calculated. Figures 9a-d depict the variations of the correlation dimension for the monthly scaled time series and Figs. 10a-d show its variation for the weekly scaled series. Both figures contain the variations of the correlation dimension for the original signals and the DWT based de-noised signals. Results indicate that while the noisy original signals for both weekly and monthly scale show low evidence of chaos, DWT based approximation signals reach a saturation value at a defined embedding dimension which indicates the

existence of chaos. Khatibi et al. (2012) have come to the same result while investigating chaos in river discharge [47].

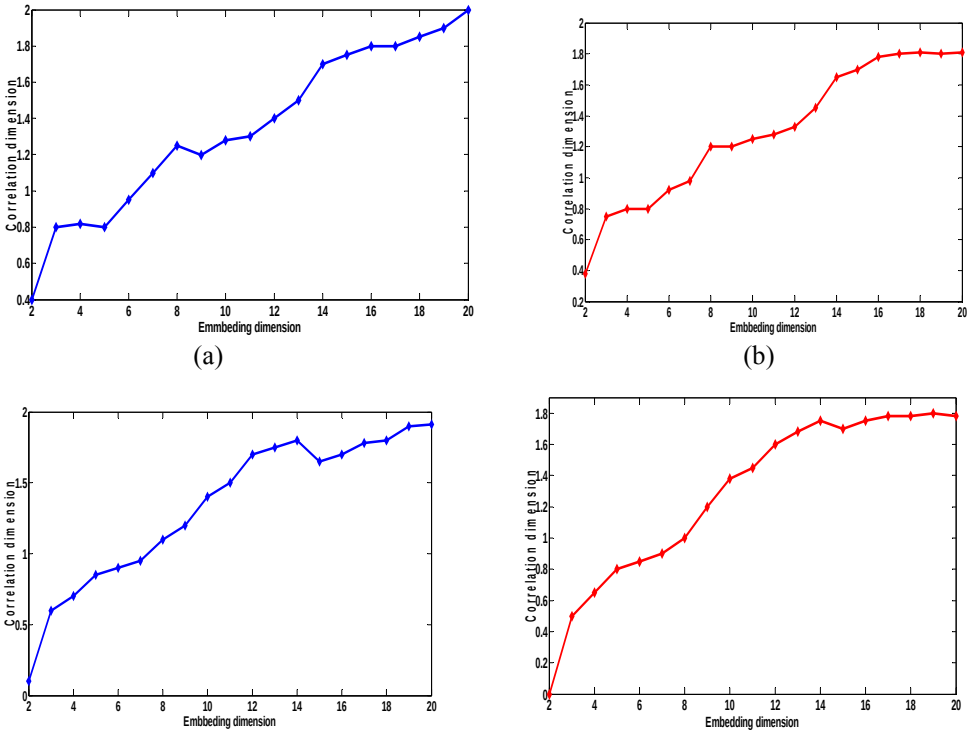

Fig. 9. Variation of correlation exponent with the embedding dimension (a) Monthly scaled original signal of Band-e-Bahman station (b) Monthly scaled DWT based app. Signal of Band-e-Bahman. (c) Monthly scaled original signal of Aliabad station. (d) Monthly scaled DWT based app. Signal of Aliabad station

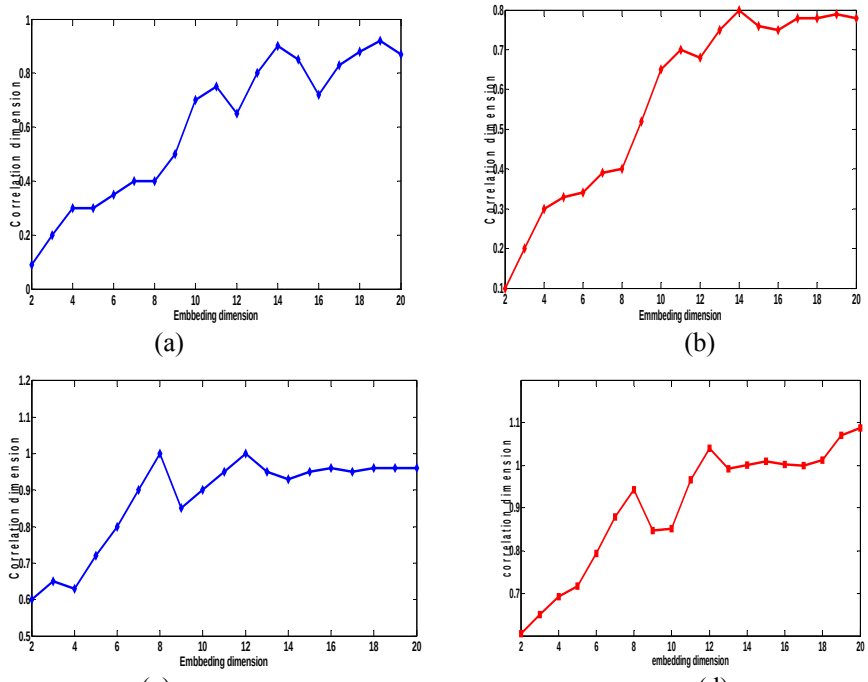

Fig. 10. Variation of correlation exponent with the embedding dimension (a) Weekly scaled original signal of Band-e-Bahman station (b) Weekly scaled DWT based app. Signal of Band-e-Bahman. (c) Weekly scaled original signal of Aliabad station (d) Weekly scaled DWT based app. Signal of Aliabad station

While the correlation dimension kept growing linearly with increasing the embedding dimension for the original signals, the value of the correlation dimension for the de-noised signals leveled off after a certain embedding dimension. It can be concluded that noise reduction can efficiently change the random behaviors of natural time series into chaotic behaviors as well as enhancing their predictability.

4. CONCLUSION

Chaotic assessments have been performed in order to evaluate the influence of the WT preprocessing techniques on the inherent behavior of hydrological time series. Wavelet de-noising approach using CWT and DWT techniques was employed in order to preprocess the data series.

It was emphasized that a crucial step in implementation of this method is the determination of noise level as well as the standard deviation of noise. The estimated noise level and the standard deviation of noise can then be utilized to assure that the clean (original) time series is not corrupted during de-noising. Removal of details having a standard deviation higher than that of the estimated noise can result in loss of important information present in time series. A prior knowledge of noise level can considerably enhance efficiency of the presented technique. Among a number of noise level estimation methods which have been presented to date, Gaussian kernel algorithm was considered and utilized. The mentioned technique had a reasonable accuracy. Therefore, noise level was estimated and used as an important criterion to control the results of de-noising and to determine the number of wavelet based de-noising stages.

Noise reduction resulted in a significant change in time series chaotic behavior. The average signal power variation due to decomposition (de-noising) procedure was remarkable. Results indicated that a considerable amount of the signal's total energy can be attributable to the signal's noise content. This amount of energy is revealed in the form of irregularities like jumps and sharp spikes in the signal [48-49]. The chaotic behavior of signals and their phase space pattern were also under the influence of de-noising. Results indicated a decrease in the random behavior of the phase space and an increase in the chaotic behavior. Lyapunov exponent, as a major chaotic criterion, was also influenced by the preprocessing. Results depicted a direct relationship between excluding the noise components of signals and a decrease in the Lyapunov exponents. Correlation dimension varied significantly under the influence of noise which confirms its efficiency as a noise indicator. Moreover, for the de-noised time series, fractal dimension and the correlation dimension were almost the same, though they were completely different before de-noising. Results depicted that while original time series had almost completely random behavior according to the correlation dimension analysis, de-noised time series showed an evident chaotic behavior.

Chaotic assessment of time series after applying the wavelet based de-noising revealed the potential capabilities of this technique for time series preprocessing. Noise reduction was understood to be an important stage in studying the chaotic behavior of the time series as it was seen that natural time series may have completely different behavior than what could be considered first. Therefore, suitable analyzing tools are needed to reveal the real behavior. Wavelet based de-noising technique was found to be an efficient approach to disclose the inherent chaotic nature of natural phenomena.

Acknowledgment: Authors would like to express their sincere gratitude to Marvdasht Islamic Azad University which has supported this research and also Mrs. Azam Bamdad for her valuable comments.

REFERENCES

1. Kawamora, A., McKerchar, A., Spigel, R. H. & Jinno, K. (1998). Chaotic characteristics of the southern oscillation index time series. *Journal of Hydrology*, Vol. 204, pp. 168-181.

2. Lotric, U. & Dobnikar, A. (2005). Predicting time series using neural networks with wavelet based de-noising layers. *Neural Computations and Applications*, Vol. 14, pp. 11-17.
3. Elshorbagy, A., Simonovic, S. P. & Panu, U. S. (2002). Noise reduction in chaotic hydrologic time series: facts and doubts, *Journal of Hydrology*, Vol. 256, pp. 147-165.
4. Grassberger, P., Schreiber, I. & Schaffrath, C. (1991). Non-linear time sequences analysis. *Int. Journal of Bifurc. Chaos*, Vol. 1, pp. 521-547.
5. Sivakumar, B. (2000). Chaos theory in hydrology: important issues and interpretations. *Journal of Hydrology*, Vol. 227, pp. 1-20.
6. Gerstner, T., Helfrich, H. P. & Kunoth, A. (2003). *Wavelet analysis of geoscientific data dynamics of multiscale earth systems*. Springer, pp. 70-88.
7. Cannas, B., Fanni, A., See, L. & Sias, G. (2006). Data preprocessing for river flow forecasting using neural networks: Wavelet transforms and data partitioning. *Physics and Chemistry of the Earth*, Vol. 31, pp. 1164–1171.
8. Georgakakos, K. P., Sharif, M. B. & Sturdevant, P. L. (1995). *Analysis of high resolution rainfall data*. In: Kundzewicz, Z.W. (Ed.). New uncertainty concepts in hydrology and water resources. Cambridge university press, pp. 114-120.
9. Puente, C. E. & Obegon, N. (1996). Deterministic geometric representation of temporal rainfall: results for a storm in Boston. *Water Resources Research*, Vol. 32, No. 9, pp. 2825-2839.
10. Sangoyomi, T. B., Lall, U. & Abarbanel, H. D. I. (1996). Non-linear dynamics of the great Salt Lake: dimension estimation, *Water Resources Research*, Vol. 25, No. 7, pp. 1667-1675.
11. Waelbroeck, H., Lopez-Pena, R., Morales, T. & Zertuche, F. (1994). Prediction of tropical rainfall by local phase space reconstruction *J. Atoms. Sci*., Vol. 51, No. 22, pp. 3360-3364.
12. Islam, M. N. & Sivakumar, B. (2002). Characterization and prediction of runoff dynamics: a nonlinear dynamical view. *Adv. Water Resources*, Vol. 25, pp. 179–190.
13. Jayawardena, A.W. & Lai, F. (1994). Analysis and prediction of chaos in rainfall and stream flow time series. *Journal of Hydrology,* Vol. 153, pp. 23–52.
14. Liu, Q., Islam, S., Rodriguez-lturbe, I. & Le, Y. (1998). Phase-space analysis of daily stream flow: characterization and prediction, Adv. *Water Resources*, Vol. 21, pp. 463–475.
15. Porporato, A. & Ridolfi, L. (1996). Clues to the existence of deterministic chaos in river flow. *Int. J. Mod. Phys. B,* Vol. 10, No. 15, pp. 1821–1862.
16. Porporato, A. & Ridolfi, L. (1997). Nonlinear analysis of river flow time sequences. *Water Resources Research*, Vol. 33, No. 6, pp. 1353–1367.
17. Sivakumar, B. (2004). Chaos theory in geophysics: past, present and future. *Chaos, Soliton & Fractals*, Vol. 19, pp. 441-462.
18. Krasovskaia, I., Gottschalk, L. & Kundzewicz, Z. W. (1999). Dimensionality of Scandinavian river flow regimes. *Hydrol. Sci. J*., Vol. 44, No. 5, pp. 705–723.
19. Stehlik, J. (1999). Deterministic chaos in runoff series. *J. Hydraul. Hydromech*, Vol. 47, No. 4, pp. 271–287.
20. Wang, Q. & Gan, T. Y. (1998). Biases of correlation dimension estimates of stream flow data in the Canadian prairies. *Water Resources Research*, Vol. 34, 9, pp. 2329–2339.
21. Rakhshandehroo, G. R. & Ghadampour, Z. (2011). A combination of fractal analysis and artificial neural network to forecast groundwater depth. *Iranian Journal of Science and Technology, Transaction B: Engineering*, Vol. 35, No. C1, pp. 121-130.
22. Jayawardena, A. W. & Gurung, A. B. (2000). Noise reduction and prediction of hydrometrological time series: dynamical system approach vs. stochastic approach. *Journal of Hydrology*, Vol. 228, pp. 242-264.
23. Lisi, F. & Villi, V. (2001). Chaotic forecasting of discharge time series: a case study. *J. Am. Water Resour. Assoc*., Vol. 37, No. 2, pp. 271-279.

24. Sivakumar, B. (2003). Forecasting monthly stream flow dynamics in the western United States: a non-linear dynamical approach, *Environmental modeling and software*, pp. 18721-728.
25. Nason, G. P. & Von Sachs, R. (1999). Wavelets in time series analysis. *Philosophical Transactions of the Royal Society of London. series A*, Vol. 357, pp. 2511–2526.
26. Mandelbrot, B. B. & Van Ness, J. W. (1968). Fractional Brownian motions, fractional noises and applications. *SIAM Rev*., Vol. 10, pp. 422-437.
27. Fattahi, M. H., Talebbeydokhti, N., Rakhshandehroo, G. R., Shamsai, A. & Nikooee, E. (2010). The robust fractal analysis of the time series- concerning signal class and data length. *Fractals*, Vol. 9, pp. 1-21.
28. Jun Zhang, K. C., Lam, Gao Yan Hang, W. J. & Yuan, L. (2004). Time series prediction using Lyapunov exponents in embedding phase space. *Computers and Electrical Engineering*, Vol. 30, pp. 1–15.
29. Sivakumar, B. (2002). A phase space reconstruction approach to prediction of suspended sediment concentration in rivers. *Journal of Hydrology*, Vol. 258, pp. 149-162.
30. Packard, N. H., Crutchfield, J. P., Farmer, J. D. & Shaw, R. S. (1980). Geometry from a time series. *Phys. Rev. Letters*, Vol. 45, No. 9, pp. 712-718.
31. Moon, F. C. (2004). *Chaotic and fractal dynamics: an introduction for applied scientists and engineers*. WILEY-VCH Verlag GmbH & Co. KGaA, Weinheim, pp. 77-78.
32. Rosenstein, M. T., Collins, J. J. & De Luca, C. J. (1993). A practical method for calculating largest Lyapunov exponents from small data sets. *Physica D*, Vol. 65, pp. 117-134.
33. Cao, L. (1997). Practical method for determining the minimum embedding dimension of a scalar time series. *Physica D*, Vol. 110, pp. 43-50.
34. Serletis, A., Shahmoradi, A. & Serletis, D. (2007). Effect of noise on estimation of Lyapunov exponents from a time series. *Chaos, Solitons and Fractals*, Vol. 32, pp. 883–887.
35. Dhanya, C. T. & Nagesh Kumar, D. (2010). Nonlinear ensemble prediction of chaotic daily rainfall. *Adv. Water Resources*, Vol. 33, No. 3, pp. 327-347.
36. Grassberger, P. & Procaccia, I. (1983). Measuring the strangeness of the strange attractors. *Physica D*, Vol. 9, pp. 189-208.
37. Schreiber, T. (1993). Extremely simple noise reduction method. *Phys Rev E*, Vol. 47, pp. 2401-2404.
38. Schouton, J. C., Takens, F. & van den Bleek, C. M. (1994). Estimating of the dimension of a noisy attractor. *Phys Rev E*, Vol. 50, pp.1851-1862.
39. Smith, L. A. (1992). Identification and prediction of low dimensional dynamics. *Physica D*, Vol. 58, pp. 50-76.
40. Diks, C. (1996). Estimating invariance of noisy attractors. *Phys Rev E*, Vol. 53, No. 5, pp. 4263-4266.
41. Yu, D., Small, M., Harrison, R.G., Diks, C. (2000). Efficient implementation in estimating invariance and noise level from time series data. *Phys Rev E*, Vol. 61, No. 4, pp. 3750-3756.
42. Argyris, J., Andreadis, L., Pavlos, G. & Athanasiou, M. (1998). On the influence of noise on the largest Lyapunov exponent and on the geometric structure of attractors. *Chaos, Solitons and Fractals*, Vol. 9, No. 6, pp. 947-958.
43. Argyris, J. & Andreadis, L. (1998). On linearisable noisy systems. *Chaos, Solitons and Fractals*, Vol. 9, No. 6, pp. 895-899.
44. Hai-Feng, L., Zheng Hou, D., Wei-Feng, L., Xin, G. & Zun Hong, Y. (2005). Noise robust estimates of the largest Lyapunov exponents. *Physics Letters A*, Vol. 341, pp. 119-127.
45. Ott, E. (1993). *Chaos in dynamical systems*. 1st ed. Cambridge University Press. Cambridge, MA.
46. Wang, L. & Garnier, H. (2012). *System identification, environmental modeling and control system design*. chapter 26, Chaos Theory for Modeling Environmental Systems: Philosophy and Pragmatism, Bellie Sivakumar, Springer-Verlag London Limited, pp. 533-556.
47. Khatibi, R., Sivakumar, B., Ghorbani, M.A., Kisi, O., Kocak, K. & Farshidizadeh, D. (2012). Investigating chaos in river stage and discharge time series. *Journal of Hydrology*, Vol. 414-415, pp. 108-117.

48. Fattahi, M. H., Talebbeydokhti, N., Rakhshandehroo, G. R., Shamsai, A. & Nikooee, E. (2011). Fractal assessment of wavelet based techniques for improving the predictions of the artificial neural network. *Journal of Food, Agriculture & Environment*, Vol. 9, No. 1, pp.719-724.
49. Fattahi, M. H., Talebbeydokhti, N., Rakhshandehroo, G. R., Shamsai, A. & Nikooee, E. (2011). Fractal assessment of wavelet based pre-processing methods for river flow time series. *Journal of Water Resources Engineering* (in Farsi), Vol. 5, pp.1-8.